THE JOURNAL OF PHYSICAL CHEMISTRY B

ARTICLE

pubs.acs.org/JPCB

# π-Conjugation of Two Nitronyl Nitroxides-Attached Diarylethenes

Satoshi Yokojima,*[,†,‡] Takao Kobayashi,[§] Keiko Shinoda,[§] Kenji Matsuda,[∥] Kenji Higashiguchi,[∥] and Shinichiro Nakamura*[,†,‡]

[†]Nakamura Laboratory, RIKEN, 2-1 Hirosawa, Wako, Saitama 351-0198, Japan

[‡]The KAITEKI Institute, Inc., 14-1 Shiba 4-chome, Minato-ku, Tokyo 108-0014 Japan

[§]Mitsubishi Chemical Group Science and Technology Research Center, Inc., 1000 Kamoshida-cho, Aoba-ku, Yokohama 227-8502, Japan

[∥]Department of Synthetic Chemistry and Biological Chemistry, Graduate School of Engineering, Kyoto University, Katsura, Nishikyo-ku, Kyoto 615-8510, Japan

Supporting Information

**ABSTRACT:** Unusual blue shift of the absorption maxima of two nitronyl nitroxide attached diarylethene through phenyl units (DAE-phe-NN) with increasing number of phenyl units is examined by time dependent density functional theory (TDDFT). The extended π-conjugation between nitronyl nitroxide and diarylethene is rather suppressed by the bridge phenyl units. In comparison, the red shift found in two nitronyl nitroxide attached diarylethenes through thiophene units (DAE-thio-NN) with increasing number of thiophene units is due to the longer π-conjugation induced by smaller dihedral angles between diarylethene and bridge and between bridges.

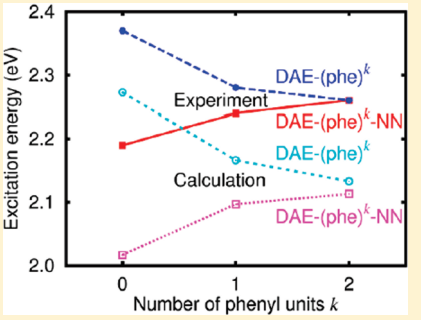


## 1. INTRODUCTION

The conjugation length (coherence size) in materials and molecules has attracted much attention for a long time.[1] From the material point of view, the exciton radius in bulk system, which corresponds to the coherence size, is shortened by reducing the system size. This is called quantum confinement. In molecular systems, the conjugation length is in parallel with the system size for a small molecule but is saturated to one value with increasing the system size.[2] The saturation of the conjugation length affects the various physical properties. For example, a red shift in absorption peak is typically observed with increasing the system size.[3]

Unlike the usual red shift, we previously found a system that showed a blue shift with increasing system size.[4] The system is a derivative of diarylethene (DAE).[4,5] One of the reported examples of the blue shift in absorption spectra with increasing the system size was found in H-aggregate systems.[6] In that case, a large transition dipole appears at the highest energy of the split excited states and transition dipoles of other low-lying excited states disappear due to the cancellation of the transition dipole of each unit. This is due to the special molecular arrangement; i.e., the transition dipole of each unit is perpendicular to the direction of the increase of the system. In the derivative of diarylethene, the system size increases along the direction of transition dipole. Thus, the blue shift observed in our system is not interpreted by the mechanism found in H-aggregate.

DAE shows photochromism as shown in Scheme 1. It is one of the promising candidates for a molecular switch due to its thermal stability of two isomers, i.e., open-ring isomer **1a** and closed-ring isomer **1b** (Scheme 1) and their fatigue-resistance.[7] To use it as a molecular switch, however, it is crucial to understand the conjugation length of the derivatives.

The series of molecules which showed the blue shift in the absorption spectra are two nitronyl nitoroxides (NN) attached closed-ring isomer of DAE through bridge phenyl unit (**2b**, **3b**, and **4b** in Charts 1). We denote these series as DAE-(phe)$^k$-NN where $k$ is the number of phenyl unit. Interestingly, the red shift was observed for the series of molecules **2b**, **5b**, and **6b** (Charts 1) where the thiophene unit instead of the phenyl unit was used as the bridge between DAE and NN.[8] (This series is denoted as DAE-(thio)$^k$-NN.) These DAE-(phe)$^k$-NN and DAE-(thio)$^k$-NN have very small singlet−triplet energy gap.[4,5,8] In contrast, as is easily expected for the system without NN, the red shift was observed for the series of molecules **1b**, **7b**, and **8b** (Charts 2),[4] which is denoted as DAE-(phe)$^k$.

To understand the mechanism of the blue shift in the absorption spectra of two nitronyl nitroxides attached diarylethenes with increasing the system size, we synthesized the molecules **9b** and **10b** (DAE-(thio)$^k$ shown in Charts 2) and

**Special Issue:** Shaul Mukamel Festschrift

**Received:** January 10, 2011
**Revised:** March 12, 2011
**Published:** March 28, 2011

compared the effect of phenyl units to that of thiophene units on the absorption spectrum. We further performed calculations by density functional theory[9] (DFT) and time dependent DFT[10] (TDDFT) with the broken symmetry method[11] for singlet biradical ground and excited states. The obtained excitation energies reproduce the blue shift of the absorption spectrum of DAE-(phe)$^k$-NN and the red shifts of the absorption spectrum of DAE-(phe)$^k$, DAE-(thio)$^k$, and DAE-(thio)$^k$-NN.

To understand those shifts in the absorption spectrum, we analyzed the orbital energies as well as the dependence on the dihedral angle between the DAE and the phenyl (thiophene) unit. We found that the experimental absorption around 2.1−2.4 eV is primarily due to the transition between the highest occupied molecular orbital (HOMO) and the lowest unoccupied molecular orbital (LUMO). The energy gaps between HOMO and LUMO correlate with the excitation energies. By analyzing these energy gaps and orbitals, we attribute the blue shift in absorption spectrum to the suppression of a large $\pi$-conjugation between DAE and NN by inserting the phenyl unit.

## 2. EXPERIMENTS

Molecules **9a** and **10a** (Scheme 2) were prepared from **1a**, 2-bis(6-iodo-2-methyl-1-benzothiophene-3-yl)hexafluorocyclopentene[4] using Suzuki coupling with 2-thiopheneboronic acid or 2-(2,2′-bithiophen-5-yl)-4,4,5,5-tetramethyl-1,3,2-dioxaborolane. $^1$H NMR spectra were recorded on a JEOL JMN-A500 instrument and mass spectra were obtained by a ThermoFisher Scientific EXACTIVE APCI mass spectrometer. Purification was carried out using a HPLC (HITACHI LC System LaChrom) with a semipreparative column (Wako Wakosil 5SIL $\phi$10 × $l$250 mm). A JASCO V-670 spectrometer was used to obtain UV−vis spectra. Photoirradiation was carried out using a USHIO 500 W super high-pressure mercury lamp by passing the light through a combination of band-pass filter (ATG UV-D33S) and monochromator (Ritsu MC-20 L).

**1,2-Bis(6-(2-thienyl)-2-methyl-1-benzothiophene-3-yl)-hexafluorocyclopentene (9a).** Colorless oil. $^1$H NMR (TMS, 500 MHz, $CDCl_3$): $\delta$ 1.54 (s, 3.9H, antiparallel), 2.21 (s, 2.1H, parallel), 7.0−7.7 (m, 10H), 7.82 (s, 0.7H, parallel), 7.91 (s, 1.3H, antiparallel). UV−vis (EtOAc) $\lambda_{max}$ 311 nm. APCI HRMS ($m/z$) $[M + H]^+$ calcd for $C_{31}H_{19}F_6S_4$: 633.0268. Found: 633.0271.

**1,2-Bis(6-(5-(2-thienyl)-2-thienyl)-2-methyl-1-benzothiophene-3-yl)hexafluorocyclopentene (10a).** Pale-yellow oil. $^1$H NMR (TMS, 500 MHz, $CDCl_3$): $\delta$ 1.56 (s, 3.7H, antiparallel), 2.25 (s, 2.3H, parallel), 7.0−7.7 (m, 14H), 7.84 (s, 0.8H, parallel), 7.93 (s, 1.2H, antiparallel). UV−vis (EtOAc): $\lambda_{max}$ 355 nm. APCI HRMS ($m/z$) $[M + H]^+$ calcd for $C_{39}H_{23}F_6S_6$: 797.0023. Found: 797.0001.

## 3. COMPUTATIONAL METHODS

The ground state structures were optimized by restricted DFT (for **1b** and **7b**−**10b**) and unrestricted DFT (UDFT) (for **2b**−**6b**) with the B3LYP[12] exchange−correlation functional. The excited states were calculated by the TDDFT (for **1b** and **7b**−**10b**) and unrestricted TDDFT (TDUDFT) (for **2b**−**6b**) with the B3LYP exchange−correlation functional. Throughout these calculations, the 6-31G(d) basis set was

**Scheme 1**

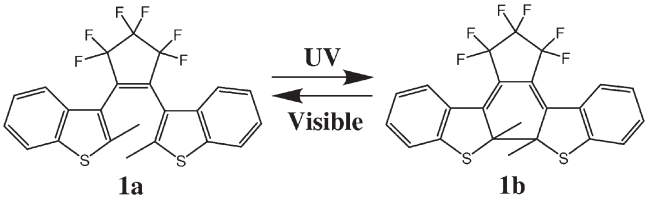


**Chart 1**

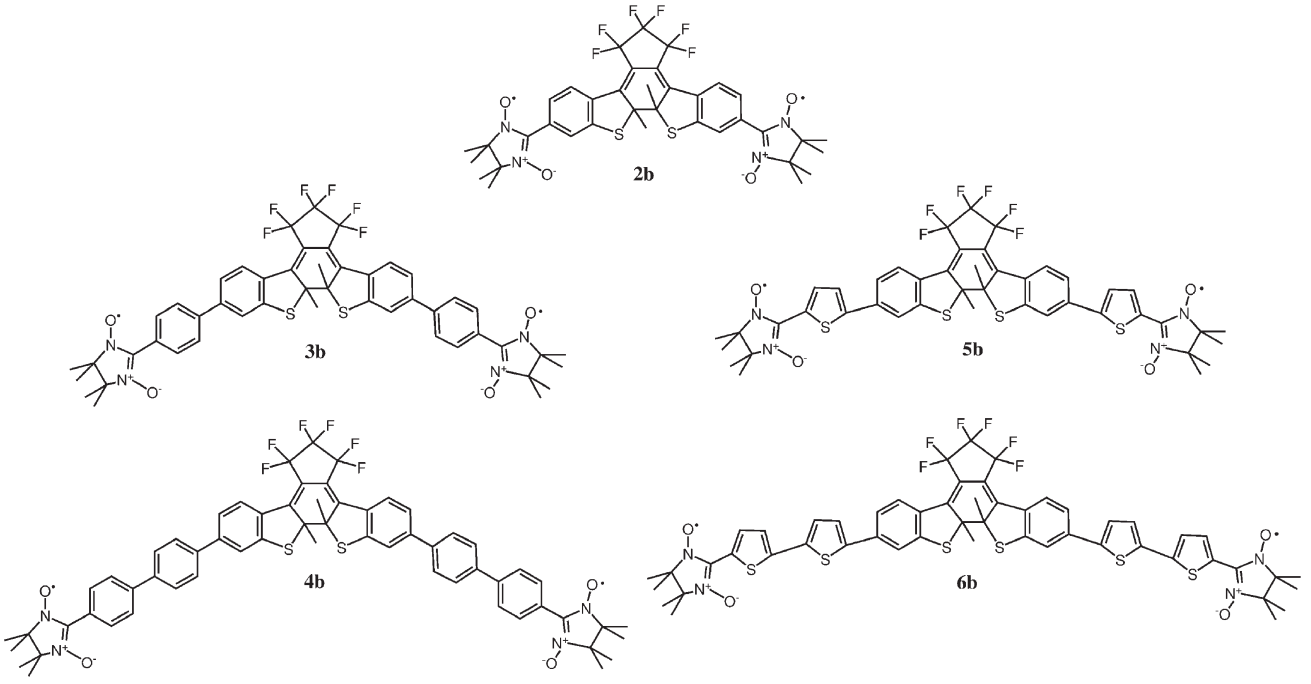



dx.doi.org/10.1021/jp2002707 |J. Phys. Chem. B 2011, 115, 5685–5692

Chart 2

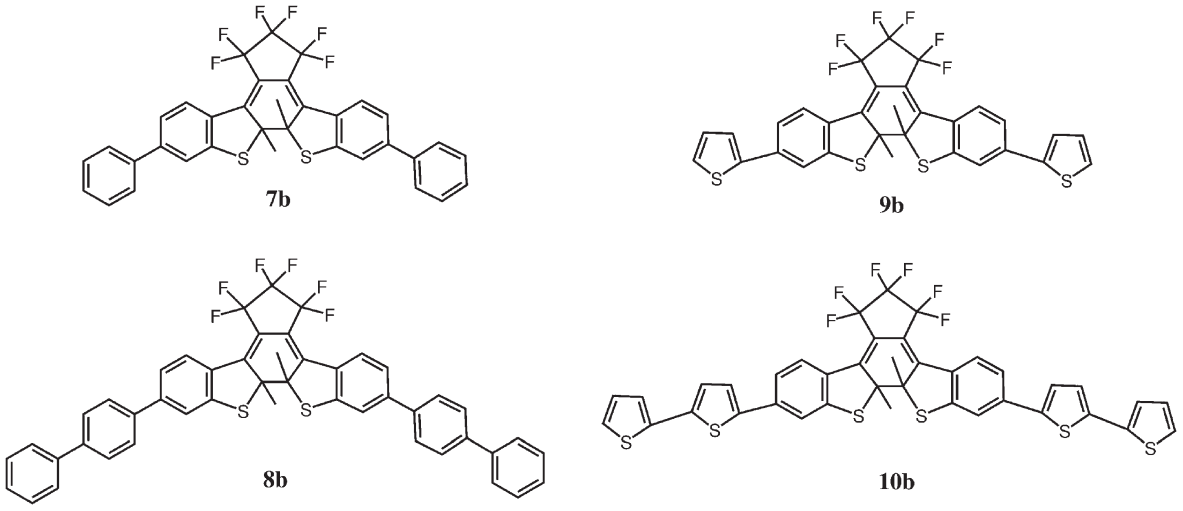


Scheme 2

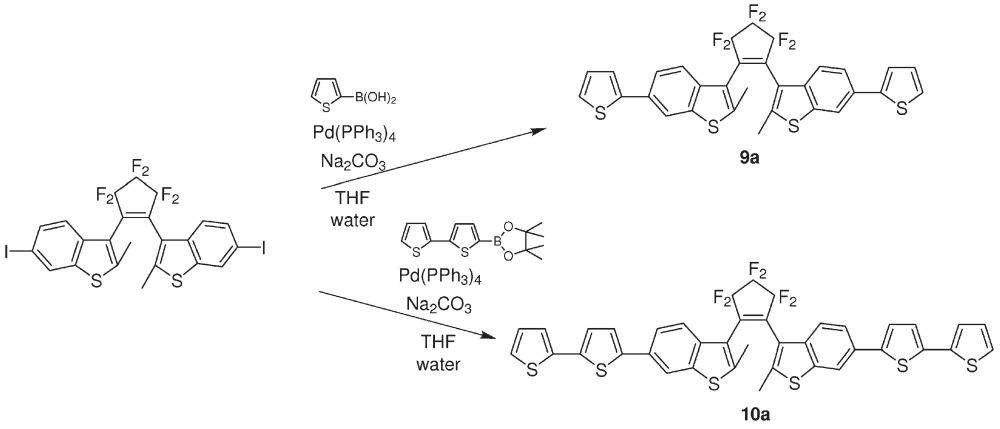


used and $C_2$ symmetry was imposed. As we have previously examined, the imposed symmetry does not affect the results.[13] The NN is a stable radical. It was observed from EPR that DAE-NN (**2b**−**6b**) has a very small singlet−triplet energy gap.[4,5,8] The open-shell singlet biradical state was obtained at the broken-symemtry[11] (BS-)UDFT level. The energy corrections by spin-projection for those results are unnecessary due to the small exchange interaction between two radical spins even for **2b** ($J = -0.5 \times 10^{-3}$ eV), which was obtained by EPR.[5a] To further confirm our conclusion, we performed additional calculations by two long-range corrected functionals, i.e., CAM-B3LYP[14] and LC-BLYP.[15] For the analysis of molecular orbital energies, we adopted Kohn−Sham orbital energies as approximate molecular orbital energies. All the calculations were performed by Gaussian 09.[16]

## 4. RESULTS AND DISCUSSION

To compare the effect of phenyl units to that of thiophene units on the shift of absorption spectrum, the absorption spectra of **9** and **10** were obtained (Figure 1). The new absorption peaks found in the photostationary state upon irradiation with UV light are due to the absorption of product of photoreaction, i.e., the closed-ring isomer **9b** and **10b** for Figure 1a,b, respectively. The absorption peaks are at 559 nm (2.22 eV) and 578 nm (2.15 eV) for **9b** and **10b**, respectively. These results together with our previous experimental results for **1b**−**8b**[4,5,8] are summarized in Figure 2. The absorption peaks of DAE-(phe)$^k$-NN showed the blue shift. In contrast, the red shift was observed for DAE-(thio)$^k$-NN. Both DAE-(phe)$^k$ and DAE-(thio)$^k$ showed red shifts, but the shift was much larger in DAE-(thio)$^k$. In both cases, the energy of the absorption peak seems to converge to one value with increasing the number of bridge unit. The experimental shifts were nicely reproduced by the computational excitation energies (Figure 2), although all the excitation energies were underestimated. To confirm that these results were not affected by the deficiency of B3LYP exchange−correlation functional, the long-range corrected functionals (CAM-B3LYP and LC-BLYP) were used to optimize the geometry and to obtain the excited states (Figures S1 and S2, Supporting Information). Those functionals significantly overestimated the excitation energies, however, the blue shifts were reproduced.


dx.doi.org/10.1021/jp2002707 |J. Phys. Chem. B 2011, 115, 5685–5692

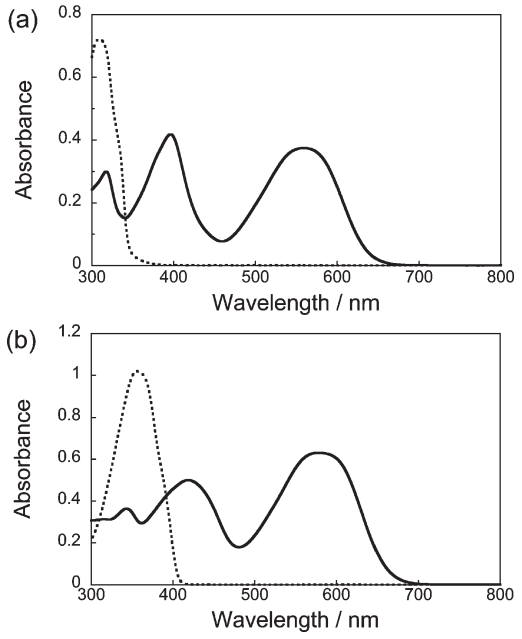


**Figure 1.** (a) Absorption spectra of **9** in ethyl acetate: open-ring isomer **9a** (dotted line) and in the photostationary state upon irradiation with 313 nm light (solid line). (b) Absorption spectra of **10** in ethyl acetate: open-ring isomer **10a** (dotted line) and in the photostationary state upon irradiation with 365 nm light (solid line).

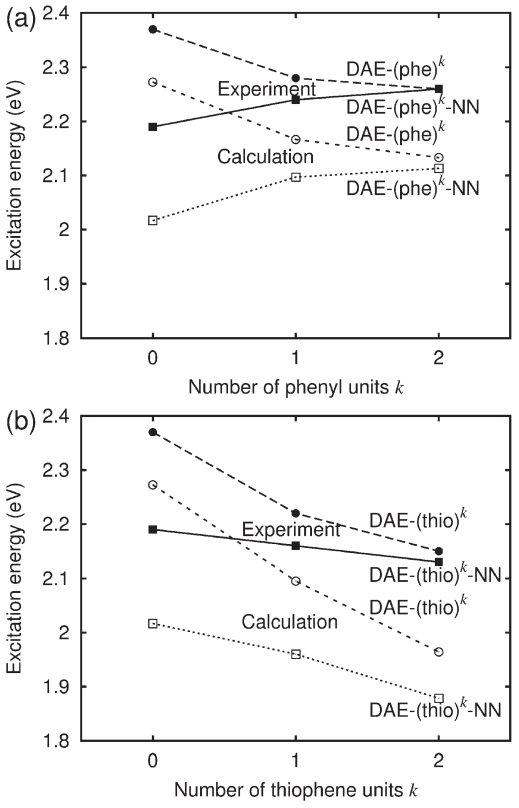


**Figure 2.** Number of $\pi$-conjugated bridge units ($k$) dependence of the excitation energies. The bridge units are (a) phenyl units and (b) thiophene units. Solid lines with filled squares: experimental excitation energies for DAE-(phe)$^k$-NN in (a) and DAE-(thio)$^k$-NN in (b). Long dashed lines with filled circles: experimental excitation energies for DAE-(phe)$^k$ in (a) and DAE-(thio)$^k$ in (b). Dotted lines with open squares: computational excitation energies for DAE-(phe)$^k$-NN in (a) and DAE-(thio)$^k$-NN in (b). Short dashed lines with open circles: computational excitation energies for DAE-(phe)$^k$ in (a) and DAE-(thio)$^k$ in (b).

To understand the mechanism of the blue shift, we further calculated the potential energy surface by imposing a constraint on the dihedral angle between the DAE and phenyl unit of the DAE-phe-NN (Figure 3) and between the DAE and thiophene unit of the DAE-thio-NN (Figure 4). In addition, $C_2$ symmetry was imposed for the simplicity. Other degrees of freedom in the structures were fully optimized. Due to the imposed $C_2$ symmetry, two dihedral angles between DAE and bridge rotate together. Thus, we need to note that the energy barriers (at around $\pm 90°$) between two local minima shown in Figures 3 and 4 are about twice the actual energy barrier for the rotation of one dihedral angle between DAE and phenyl (thiophene) unit.

The dihedral angle between the DAE and the bridge at the ground state depends on the bridge. The dihedral angle between DAE and the phenyl (thiophene) unit at the ground state is 35 (22)°. The difference between the two dihedral angles is due to the steric hindrance between two hydrogen atoms. The same is the reason for the difference of the dihedral angle between two phenyl (thiophene) units. According to the reported crystal structure, the angle between two phenyl rings of biphenyl is around 10°,[17] while two thiophene rings of 2,2′-bithiophene are coplanar.[18]

The $\pi$-conjugation is thus less extended in DAE-(phe)$^k$-NN than in DAE-(thio)$^k$-NN. The larger dihedral angle between DAE and phenyl unit suppresses the $\pi$ orbital mixing between DAE and phenyl unit. Therefore, relatively larger red shifts in DAE-(thio)$^k$-NN than in DAE-(phe)$^k$-NN may be expected. Actually, in the case without NN unit for both, the similar dihedral angle dependence is found in DAE-(phe)$^k$ and DAE-(thio)$^k$; larger red shift for DAE-(thio)$^k$ than for DAE-(phe)$^k$. The similar results were reported for many different systems.[19] However, the blue shift is found in the absorption spectra of DAE-(phe)$^k$-NN, which cannot be explained only by the dihedral angles. It suggests that there is another factor to explain the blue shift.

The number of bridge unit dependence of the Kohn−Sham orbital energies gives another insight. The Kohn−Sham orbital energies near HOMO and LUMO are shown in Figures 5 and 6. The NN attached series is shown in Figure 5 and the series without NN is shown in Figure 6. Even though unrestricted DFT calculation was performed for the NN-attached series, due to the small exchange interaction energy between two spins localized on each NN, α and $\beta$ orbital energies are degenerated. Thus, only α orbital energies are shown in Figure 5 and closed shell Kohn−Sham ones in Figure 6. The NN localized orbitals are shown in dashed lines in Figure 5. The SOMOs are localized on the NN and the orbital energies are found near −5 eV, which are quite similar to the orbital energies of the HOMO. The orbital energies of the LUMO are found around −2.8 eV. Those orbitals are shown in Figure 7. The α SOMO is localized on the left NN as shown in Figure 7c whereas the $\beta$ SOMO is symmetrically localized on the right NN. The HOMO (Figure 7d) and the LUMO (Figure 7b) are quite symmetric. Since the SOMO orbitals are quite similar due to the localization on NN, only the HOMO and LUMO are shown for the DAE-(phe)$^k$-NN (Figure 8) and the DAE-(thio)$^k$-NN (Figure 9).


dx.doi.org/10.1021/jp2002707 |J. Phys. Chem. B 2011, 115, 5685–5692

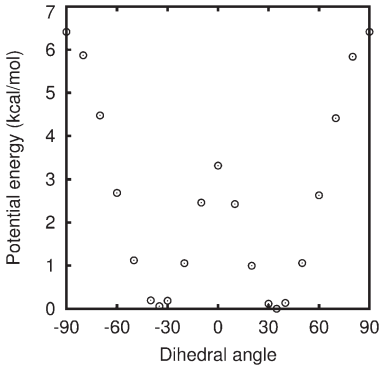


**Figure 3.** Dihedral angle dependence of the ground state potential energy (open circles) for **3b** (DAE-phe-NN).

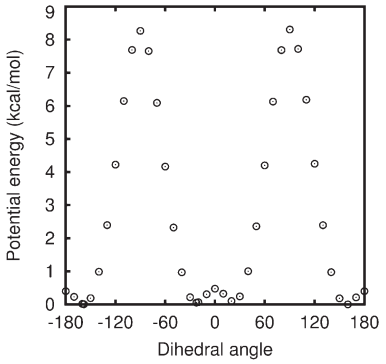


**Figure 4.** Dihedral angle dependence of the ground state potential energy (open circles) for **5b** (DAE-thio-NN).

The absorption around 2.1−2.4 eV is mainly due to the HOMO−LUMO transition. The HOMO−LUMO energy gap is usually reduced with increasing $\pi$-conjugation. The decrease of the energy gaps, which correlates with the red shift of the absorption spectrum in the DAE-$(phe)^k$ and in the DAE-$(thio)^k$, is found in Figure 6. The change of orbital energies with increasing number of phenyl or thiophene units in Figure 6 is rather simple; i.e., the HOMO energy increases and the LUMO energy decreases. In contrast, the change of the HOMO and the LUMO energies are rather complicated in Figure 5, but the change of the energy gaps are correlated with the shifts of the absorption spectrum as well.

The comparison between the HOMO (LUMO) energies of DAE ($k = 0$ in Figure 5) and DAE-NN ($k = 0$ in Figure 6) reveals that the HOMO (LUMO) energy of DAE-NN is lifted (lowered) by the large orbital mixing between DAE and NN in comparison with the HOMO (LUMO) energy of DAE. Inserting the phenyl unit between DAE and NN rather suppresses the $\pi$-conjugation, which results in the increase of the energy gap in the DAE-$(phe)^k$-NN and consequently the blue shift of the absorption spectra. As for the DAE-$(thio)^k$-NN, $\pi$-conjugation is not suppressed by the bridge thiophene unit. Therefore, the energy gap in the DAE-$(thio)^k$-NN is reduced with the increasing number of thiophene units and we found the red shift of the absorption spectrum.

The explanation of the blue shift of absorption spectra by the extent of the mixing of the Kohn−Sham orbitals between DAE and NN is further supported by Figures 7−9. The HOMO and LUMO of DAE-NN extend over the DAE and NN in Figure 7.

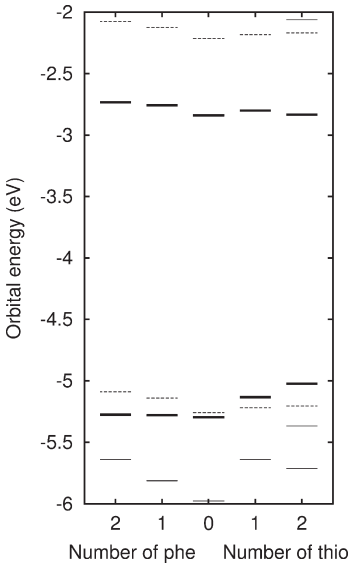


**Figure 5.** Kohn−Sham orbital energies near HOMO and LUMO for NN attached DAEs. The number of bridge units $k$ are shown on the horizontal axis. The value $k = 0$ at the center is for **2b** (DAE-NN). The left (right) hand side is for the number of phenyl (thiophene) units, i.e., from left to right: **4b**, **3b**, **2b**, **5b**, and **6b**. Each pair of thick solid lines is HOMO (lower line) and LUMO (upper line) and is responsible for the lowest energy absorption peak. The orbital shown by the dashed line is SOMO and is localized on one of two NNs. Other orbitals are shown by thin solid lines.

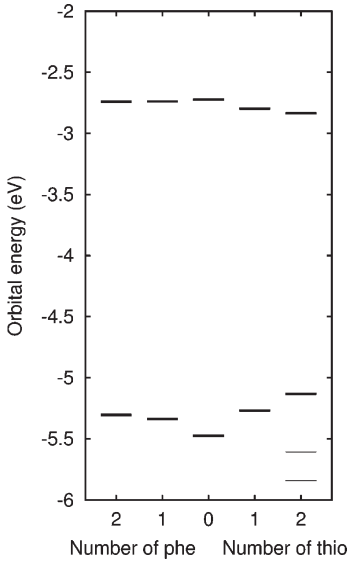


**Figure 6.** Same as Figure 5 but for DAEs without NN. From left to right: **8b**, **7b**, **1b**, **9b**, and **10b**.

Increasing the number of phenyl unit rather confines both HOMO and LUMO near the DAE (Figure 8). In contrast, the HOMO of DAE-$(thio)^k$-NN still extends over the DAE and NN through thiophene unit (Figure 9).

The large orbital mixing between DAE and NN found for the HOMO and the LUMO of DAE-NN is due to the following reasons. (i) The mixing takes place between the HOMO (LUMO) of DAE and the $\beta$-HOMO ($\alpha$-LUMO) of NN. The orbital energies of the $\beta$-HOMO and the $\alpha$-LUMO of NN are


dx.doi.org/10.1021/jp2002707 |J. Phys. Chem. B 2011, 115, 5685–5692

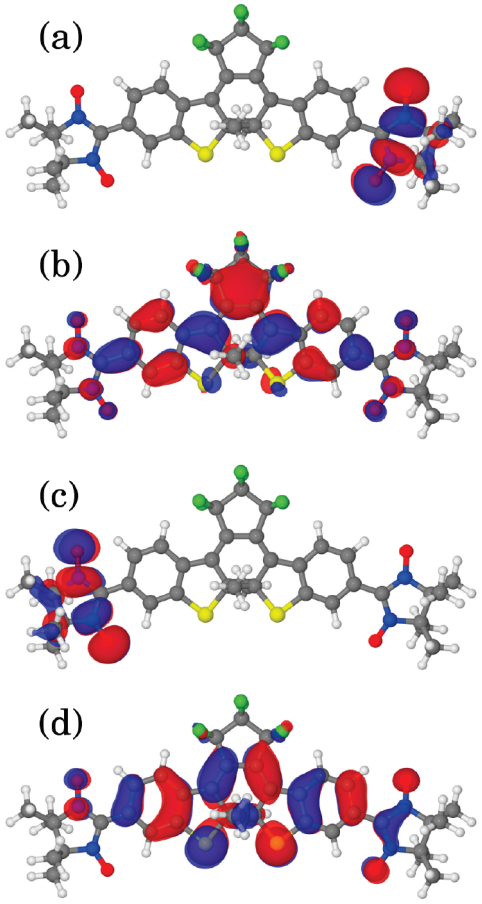


**Figure 7.** Kohn−Sham α spin orbitals for (a) LUMO+1, (b) LUMO, (c) SOMO, and (d) HOMO of **2b** (DAE-NN).

−6.20 and −0.16 eV, respectively. Those energies are closely located to the orbital energies of the HOMO (−5.47 eV) and LUMO (−2.72 eV) of DAE. In comparison, the orbital energies of the HOMO and LUMO of thiophene (benzene) are −6.33 (−6.70) eV and −0.20 (0.10) eV, respectively. The small energy difference between the HOMO of DAE and the $\beta$-HOMO of NN induces a large orbital mixing between them. (ii) The dihedral angle between DAE and NN is about 3°, which is much smaller than those between DAE and phenyl unit of DAE-phe and between DAE and thiophene unit in DAE-thio. The small dihedral angle between DAE and NN increases the mixing of the $\pi$-orbitals between them.

The extent of the mixing of the orbitals between DAE and NN through the bridge is controlled by two factors. (i) As we have seen in Figures 3 and 4, the dihedral angles between DAE and the phenyl unit as well as between phenyl units are larger than those between DAE and the thiophene unit and between thiophene units, which contributes to suppressing the mixing of the orbitals between DAE and NN. (ii) In addition, the HOMO energy of benzene is further away from that of DAE in comparison with that of thiophene. The larger orbital energy difference between DAE and benzene than that between DAE and thiophene contributes to suppressing the mixing of the orbitals between DAE and NN.

In terms of the orbital energy, the red shifts of absorption spectra in DAE-(thio)$^k$ are largely due to the destabilization of the HOMO. This is because the difference between the HOMO

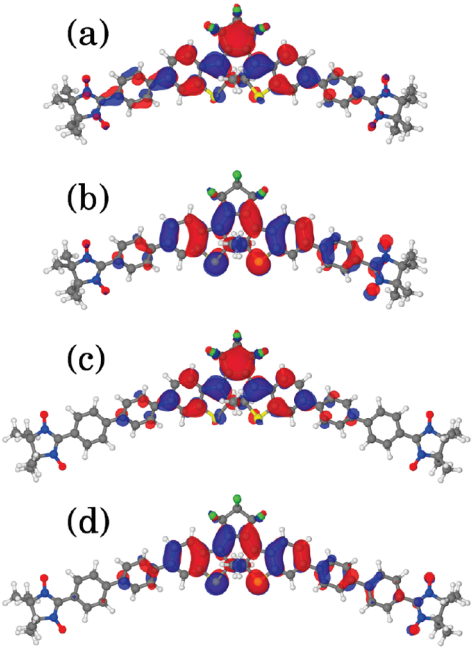


**Figure 8.** Kohn−Sham α spin orbitals for (a) LUMO and (b) HOMO of **3b** (DAE-phe-NN) and (c) LUMO and (d) HOMO of **4b** (DAE-(phe)$^2$-NN).

energy of DAE and that of thiophene is much smaller than the difference between the LUMO energy of DAE and that of thiophene. The red shift in DAE-(phe)$^k$ is similarly explained. Since the HOMO energy of benzene is lower than that of thiophene, the destabilization of the HOMO is smaller in DAE-(phe)$^k$ than in DAE-(thio)$^k$. The situation is more complicated in DAE-(phe)$^k$-NN and DAE-(thio)$^k$-NN. The HOMO energy in DAE-(phe)$^k$-NN does not change with increasing $k$ but the LUMO is destabilized, which causes the blue shift in the absorption spectrum. This is due to the fact that the HOMO is destabilized and the LUMO is stabilized by attaching NN to DAE due to the large orbital mixing between DAE and NN. Since the conjugation length is short for the phenyl group as the bridge, the orbital mixing between DAE and NN is reduced by inserting the bridge. Thus, the change of the orbital energy is determined by the trade-off between the reduction of orbital mixing between DAE and NN and the additional orbital mixing between phenyl unit and DAE. In DAE-(thio)$^k$-NN's case, the reduction of orbital mixing between DAE and NN is small and orbital mixing between thiophene and DAE is large. Consequently, the HOMO of DAE-(thio)$^k$-NN is destabilized with increasing $k$.

On the basis of these understandings, the shift in absorption spectrum in Figure 2 is interpreted as follows. The shift of absorption spectrum in DAE-(phe)$^k$ is small (0.11 eV) and saturates around $k = 2$. This indicates that the conjugation length is rather short in DAE-(phe)$^k$ and saturates around $k = 2$. Due to the large orbital mixing between DAE and NN, the absorption peak of DAE shifted toward red (0.18 eV) by attaching NN. Due to the short conjugation length of DAE-(phe)$^k$, the effect of NN is reduced in DAE-(phe)$^k$-NN with increasing $k$. Consequently, around $k = 2$ where the conjugation length saturates, the absorption peak position of DAE-(phe)$^k$-NN is similar to that of DAE-(phe)$^k$. In contrast, the shift of the absorption spectrum in DAE-(thio)$^k$ from $k = 0$ to $k = 2$ is larger than that from DAE to DAE-NN. Moreover, the red shift of the absorption spectrum in


dx.doi.org/10.1021/jp2002707 |J. Phys. Chem. B 2011, 115, 5685–5692

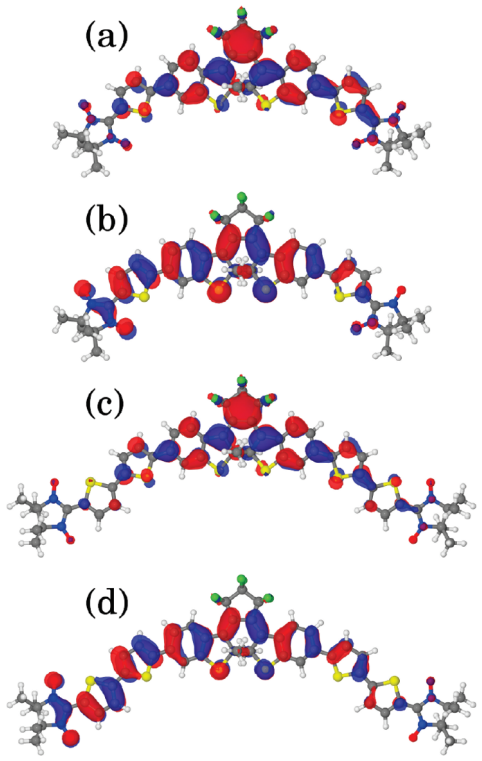


**Figure 9.** Kohn−Sham α spin orbitals for (a) LUMO and (b) HOMO of **5b** (DAE-thio-NN) and (c) LUMO and (d) HOMO of **6b** (DAE-(thio)$^2$-NN).

DAE-(thio)$^k$ with increasing $k$ does not reach the saturation at $k$ = 2. This is consistent with the long conjugated length of oligothiophenes.[20] Naturally, we observed the red shift of the absorption spectrum of DAE-(thio)$^k$-NN with increasing $k$.

One of the interesting issues about the biradical system is the effect of the quinoid structure. In our calculations, only near the NN attached bonds (about two bonds from the NN) is the effect of the quinoid-like bond lengths shown. This might be due to the limitation of the broken symmetry DFT. We also used CASSCF-(2,2) but similar results are obtained. It may be required to use larger CASSCF calculations to discuss the quinoid effect. The explanation of the blue shift in the absorption spectrum of DAE-(phe)$^k$-NN with increasing $k$, however, does not require the quinoid effect as we have seen here.

## 5. CONCLUSION

The blue shift of the absorption spectrum in DAE-(phe)$^k$-NN with increasing $k$ is explained by the orbital mixing; the large $\pi$-orbital mixing between DAE and NN is rather suppressed by the bridge phenyl units. The DAE-(thio)$^k$-NN showed the red shift of absorption spectrum because of the extended $\pi$-conjugation in DAE-(thio)$^k$-NN. This is partly due to the smaller dihedral angles between DAE and thiophene unit as well as between thiophene units in comparison with those in DAE-(phe)$^k$-NN. Additionally, the orbital energy of HOMO of DAE is closer to the HOMO energy of thiophene than that of benzene. These two effects contribute to the larger mixing of the $\pi$-orbitals through thiophene and results in the extended $\pi$-conjugation in DAE-(thio)$^k$-NN than in DAE-(phe)$^k$-NN.

## ■ ASSOCIATED CONTENT

**Supporting Information.** Complete reference of Gaussian, the computational excitation energies by CAM-B3LYP and LC-BLYP, the definition of dihedral angles in Figures 3 and 4, and the orbital energies and MOs of NN, benzene, thiophene, and DAE. This material is available free of charge via the Internet at http://pubs.acs.org.

## ■ AUTHOR INFORMATION

### Corresponding Author

*S.Y.: tel, +81-45-963-3833; fax, +81-45-963-3835; e-mail, yokojima@riken.jp. S.N.: tel, +81-45-963-3265; fax, +81-45-963-3835. e-mail, snakamura@riken.jp.

## ■ ACKNOWLEDGMENT

We thank Dr. Satoru Yamada for the discussion on the spin projection of biradical systems.

## ■ REFERENCES

(1) (a) Martin, R. E.; Diederich, F. *Angew. Chem., Int. Ed.* **1999**, *38*, 1350–1377. (b) Gierschner, J.; Cornil, J.; Egelhaaf, H.-J. *Adv. Mater.* **2007**, *19*, 173–191.

(2) (a) Mukamel, S.; Takahashi, A.; Wang, H. X.; Chen, G. *Science* **1994**, *266*, 250–254. (b) Wagersreiter, T.; Mukamel, S. *J. Chem. Phys.* **1996**, *104*, 7086–7098. (c) Mukamel, S.; Tretiak, S.; Wagersreiter, T.; Chernyak, V. *Science* **1997**, *277*, 781–787. (d) Tretiak, S.; Chernyak, V.; Mukamel, S. *Chem. Phys. Lett.* **1998**, *287*, 75–82. (e) Schulz, M.; Tretiak, S.; Chernyak, V.; Mukamel, S. *J. Am. Chem. Soc.* **2000**, *122*, 452–459. (f) Fabian, J.; Zahradník, R. *Angew. Chem., Int. Ed.* **1989**, *28*, 677–694. (g) Tolbert, L. M.; Zhao, X. *J. Am. Chem. Soc.* **1997**, *119*, 3253–3258. (h) Weil, T.; Vosch, T.; Hofkens, J.; Peneva, K.; Müllen, K. *Angew. Chem., Int. Ed.* **2010**, *49*, 9068–9093.

(3) (a) Tsuda, A.; Osuka, A. *Science* **2001**, *293*, 79–82. (b) Takahashi, T.; Matsuoka, K.-i.; Takimiya, K.; Otsubo, T.; Aso, Y. *J. Am. Chem. Soc.* **2005**, *127*, 8928–8929.

(4) Matsuda, K.; Irie, M. *Chem.—Eur. J.* **2001**, *7*, 3466–3473.

(5) (a) Matsuda, K; Irie, M. *J. Am. Chem. Soc.* **2000**, *122*, 7195–7201. (b) Matsuda, K.; Irie, M. *J. Am. Chem. Soc.* **2000**, *122*, 8309–8310.

(6) Würthner, F. *Chem. Commun.* **2004**, 1564–1579.

(7) (a) Irie, M. *Chem. Rev.* **2000**, *100*, 685. (b) Irie, M.; Uchida, K. *Bull. Chem. Soc. Jpn.* **1998**, *71*, 985.

(8) Matsuda, K.; Matsuo, M.; Irie, M. *J. Org. Chem.* **2001**, *66*, 8799–8803.

(9) (a) Hohenberg, P.; Kohn, W. *Phys. Rev. B* **1964**, *136*, B864. (b) Kohn, W.; Sham, L. J. *Phys. Rev. A* **1965**, *140*, A1133.

(10) (a) Runge, E; Gross, E. K. U. *Phys. Rev. Lett.* **1984**, *52*, 997. (b) Stratmann, R. E.; Scuseria, G. E.; Frisch, M. J. *J. Chem. Phys.* **1998**, *109*, 8218. (c) Bauernschmitt, R.; Ahlrichs, R. *Chem. Phys. Lett.* **1996**, *256*, 454. (d) Casida, M. E.; Jamorski, C.; Casida, K. C.; Salahub, D. R. *J. Chem. Phys.* **1998**, *108*, 4439.

(11) Noodleman, L. *J. Chem. Phys.* **1981**, *74*, 5737–5743.

(12) (a) Becke, A. D. *J. Chem. Phys.* **1993**, *98*, 5648. (b) Becke, A. D. *Phys. Rev. A* **1988**, *38*, 3098. (c) Lee, C.; Yang, W.; Parr, R. G. *Phys. Rev. B* **1988**, *37*, 785.

(13) Yokojima, S.; Matsuda, K.; Irie, M.; Murakami, A.; Kobayashi, T.; Nakamura, S. *J. Phys. Chem. A* **2006**, *110*, 8137–8143.

(14) Yanai, T.; Tew, D.; Handy, N. *Chem. Phys. Lett.* **2004**, *393*, 51–57.

(15) Iikura, H.; Tsuneda, T.; Yanai, T.; Hirao, K. *J. Chem. Phys.* **2001**, *115*, 3540–3544.

(16) Frisch, M. J. et al. *Gaussian 09*, Revision B.01; Gaussian, Inc.: Wallingford, CT, 2010.

(17) Cailleau, H.; Baudour, J. L.; Zeyen, C. M. E. *Acta Crystallogr. B* **1979**, *35*, 426–432.
(18) Pelletier, M.; Brisse, F. *Acta Crystallogr. C* **1994**, *50*, 1942–1945.
(19) Barigelletti, F.; Flamigni, L.; Balzani, V.; Collin, J.-P.; Sauvage, J.-P.; Sour, A.; Constable, E. C.; Thompson, A. M. W. C. *J. Am. Chem. Soc.* **1994**, *116*, 7692–7699.
(20) Izumi, T.; Kobashi, S.; Takimiya, K.; Aso, Y.; Otsubo, T. *J. Am. Chem. Soc.* **2003**, *125*, 5286–5287.